Effects of cubic carbides and La additions on WC grain morphology, hardness and toughness of WC−Co alloys

ZHANG Li[1], CHEN Shu[2], CHENG Xin[1], WU Hou-ping[1], MA Yun[1], XIONG Xiang-jun[1]

1. State Key Laboratory of Powder Metallurgy, Central South University, Changsha 410083, China;
2. Changsha Mining and Metallurgy Research Institute Co., Ltd., Changsha 410012, China

Abstract: Effects of Cr_3C_2, VC and La_2O_3 additions on the WC grain morphology, hardness and toughness of WC−10Co alloys were investigated. To intensify the grain growth driving force, nano W and nano C, instead of the conventionally used WC, were used as the starting materials. To obtain a three-dimensional WC grain morphology, the natural sinter skins of the alloys were observed directly by scanning electron microscopy. It is shown that the additions have a strong ability in regulating the WC grain morphological and grain size distribution characteristics and the combinations of hardness and toughness. Due to the formation of regular and homogeneous triangular platelet WC grains, WC−10Co−$0.6Cr_3C_2$−$0.06La_2O_3$ alloy shows an excellent combination of hardness and toughness. The morphological regulation mechanism, the relationship between the WC grain morphology and the properties were discussed.
Key words: cemented carbide; rare earth; grain growth; platelet WC grain; hardness; toughness

1 Introduction

It is well recognized that small amounts of VC and Cr_3C_2 (cubic carbides) can effectively inhibit the WC grain growth during the sintering process of ultrafine and near-nano (also called super ultrafine) WC−Co cemented carbides [1−4]. And it was reported that rare earth oxide has an ability in inhibiting the discontinuous or inhomogeneous WC grain growth in WC−Co cemented carbide at the stage of solid phase sintering [5]. Nevertheless, the WC grain growth and grain growth inhibition mechanisms still remain mysterious.

As an important component of the integrated research of the WC grain growth mechanism which is tightly related to the grain growth inhibition mechanism, we examined originally the effects of Cr_3C_2, VC and La_2O_3 additions on the microstructure and properties of WC–Co alloys under high WC grain growth driving force. The prime novelties of this work are as follows: 1) instead of the conventionally used WC powder, nano W and nano C were used as the main starting materials to intensify the grain growth driving force; 2) to keep La additions staying stably in the alloys and to avoid the effect of the foreign active elements on the crystalline morphology of WC grain on the sinter skins (surface layers), a patented furnace cleaning material was employed; 3) the sinter skins were directly observed to obtain a 3-D WC grain morphology; 4) it is revealed that Cr_3C_2, VC and La_2O_3 additions have a strong ability in regulating the WC grain morphological and grain size distribution characteristics and the related combinations of hardness and toughness. The study of the behaviors of VC, Cr_3C_2 and Ln_2O_3 (Ln: rare earth) in cemented carbides can shed more light on the understanding of the WC grain growth and grain growth inhibition mechanisms and the mechanism for determining the combination of hardness and toughness which is a common concern in cemented carbide field.

2 Experimental

2.1 Starting materials

Nano tungsten powder (Chongyi Zhangyuan

Tungsten Co., Ltd., China), nano graphite powder (TIMREX® KS4, Timcal Ltd., Switzerland), ultrafine spherical cobalt and nano lanthanum oxide powders prepared in our laboratory, and commercial chromium carbide and vanadium carbide powders were used as the starting materials. Both the chromium carbide and the vanadium carbide were pretreated for 36 h by ball milling in hexane to obtain a particle size to match the ones of other powders. The characteristics of the powders used in this study are summarized Table 1.

Table 1 Characteristics of powder materials used in this study

Powder	FSSS/ μm	S_{BET}/ (m²·g⁻¹)	d_{BET}/ nm	Total carbon content/%	Oxygen content/%
W	−	6.70	46.4	−	0.90
Co	−	2.59	255	−	0.66
C	−	26.00	106.8	−	−
La₂O₃	−	12.51	73.1	−	−
Cr₃C₂	1.02	−	−	13.26	0.50
VC	1.05	−	−	18.19	0.70

FSSS: Fischer sub-sieve size; S_{BET}: BET specific surface area; d_{BET}: BET calculated grain size; the particle sizes of Cr₃C₂ and VC are the original one before the pretreatment.

2.2 Alloy preparation and microscopic investigations

Powders corresponding to the compositions shown in Table 2 and paraffin wax based macromolecule compounds were wet-milled in a multicomponent ball-milling organic medium for 32 h in a conventional ball mill. The mass ratio of milling media (cemented carbide balls) to charge was 4:1. Dewaxing and sintering of the pressed samples were performed in a sinter-HIP furnace with controllable atmosphere. Dewaxing was carried out in H_2 from room temperature to 480 °C. Sintering was carried out in vacuum from 480 °C to 1350 °C, and then the sintering atmosphere was turned to Ar from 1350 °C to 1380 °C. At the final sintering stage of 1380 °C, Ar pressure was kept at 5.6 MPa for 40 min. After the sintering, the samples were cooled down to around 80 °C with an average cooling rate of 4−5 °C/min in Ar.

It was shown that the behavior of Ln additions in

Table 2 Composition of alloys used in this study (mass fraction, %)

Alloy	Composition
A	WC−10Co
B	WC−10Co−0.6Cr₃C₂−0.06La₂O₃
C	WC−10Co−0.6VC−0.06La₂O₃
D	WC−10Co−0.4Cr₃C₂−0.3VC−0.06La₂O₃
E	WC−10Co−0.6Cr₃C₂
F	WC−10Co−0.6VC
G	WC−10Co−0.4Cr₃C₂−0.3VC

cemented carbides is unstable. Under some conditions, e.g., a small amount of sulfur in the sintering atmosphere, Ln even added in the form of oxide can migrate directionally from the cemented carbide body to the sinter skin during the sintering process [6,7]. If Ln added stays stably in cemented carbides during the sintering process and the working environment can provide sulfur resource and moderated heat to promote the diffusion, the inward diffusion of sulfur from the sulfur-containing workpieces and the forward diffusion of Ln in the cemented carbide tools can result in the in situ formation of layer-structured Ln₂O₂S on the working surfaces [8]. As a result, Ln-containing cemented carbide tools can be endowed with a self lubricating function. In this experiment, to keep La additions staying stably in the alloys and to avoid the effect of the foreign active elements on the crystalline morphology of WC grain on the sinter skins, a patented furnace cleaning material [9] was employed. During the sintering process, the pellet cleaning material with high activity can preferentially adsorb oxygen from the sintering atmosphere as well as the volatile sulfide and other impurity elements, e.g. Ca, Si, from the carbon fiber and graphite materials in the sintering furnace.

The natural sinter skins of the samples were observed by scanning electron microscope (JEOL JSM-6490LV and JEOL JSM 5600LV) in backscattering mode to produce backscattered electrons (BSE) images.

**2.3 Vickers hardness and Palmqvist toughness tests**

Vickers hardness and Palmqvist toughness tests were performed on the polished cross section of the samples. The tests were determined according to ISO 3878: 1983 Hardmetals−Vickers hardness test and ISO 28079: 2009 Hardmetals−Palmqvist toughness test, respectively. The applied load of 294 N was chosen. The uncertainty in Vickers hardness measurement is usually in the range of ±196 N and the uncertainty in the sum of crack lengths measurement ±20 μm [10].

3 Results and discussion

3.1 Morphological characteristics of WC grains

The observation of the polished section by optical microscope shows that all the alloys A−G have a two-phase structure of WC and Co based binder phases. Figures 1(a)−(g) show the SEM micrographs of the sinter skins of alloys A−G.

It is known from Fig. 1 that the cubic carbides and La₂O₃ additions have a strong ability in regulating the WC grain morphological characteristics. For WC−10Co alloys with intensified grain growth driving force, the combination of 0.6VC−0.06La₂O₃ additions exhibits the strongest ability in suppressing the continuous WC grain
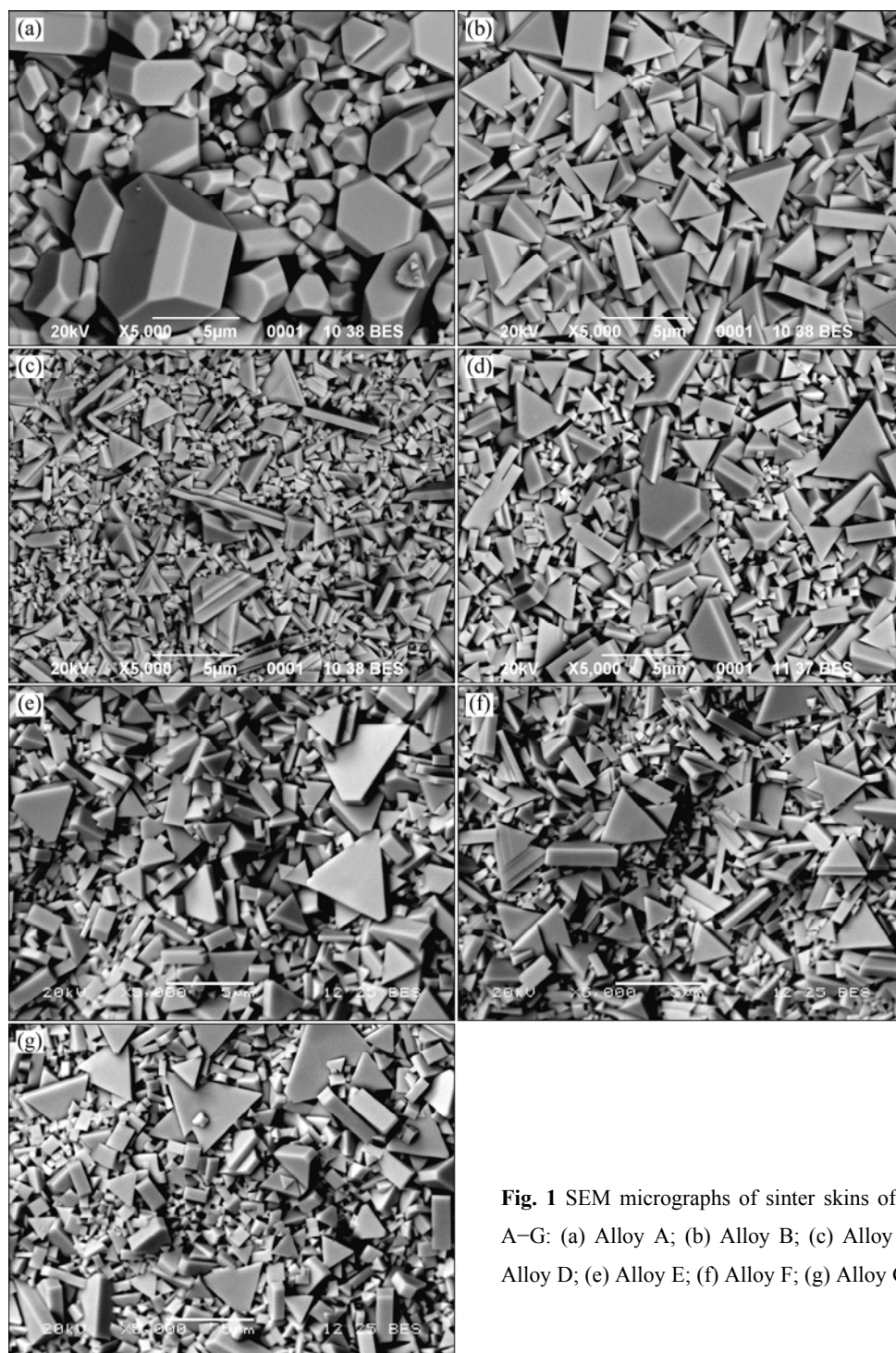
Fig. 1 SEM micrographs of sinter skins of alloys A−G: (a) Alloy A; (b) Alloy B; (c) Alloy C; (d) Alloy D; (e) Alloy E; (f) Alloy F; (g) Alloy G

growth; nevertheless, their ability in controlling the discontinuous or inhomogeneous WC grain growth is limited.

It is well established that the crystal structure of WC is simple hexagonal (type $P\bar{6}m2$). The lattice constants are a=0.2906 nm and c=0.2837 nm with a/c=1.0243 [11]. The WC grains distributed in the Co matrix usually generate three types of facets: two types of prismatic $\{10\bar{1}0\}$ facets with different spacings of the tungsten

and carbon planes, and two basal (0001) facets that delimit the flat triangular prism with truncated corners [11], as shown in Fig. 2.

From Fig. 1, it is known that the combination of $0.6Cr_3C_2-0.06La_2O_3$ additions leads to regular triangular prism WC grains. Whereas, singular $0.6Cr_3C_2$ and the combinations of $0.4Cr_3C_2-0.3VC$ and $0.4Cr_3C_2-0.3VC-0.06La_2O_3$ additions lead to a mixture of triangular and truncated triangle prism WC grains with an uncertain
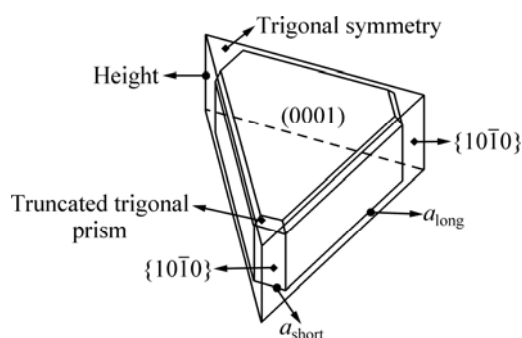
Fig. 2 Schema of equilibrium shape of WC grain in Co binder [11]

truncation factors, where truncation factor r is the ratio between the length of the two types of $\{10\bar{1}0\}$ prism facets ($r=\sum a_{short}/\sum a_{long}$) [12,13]. Singular 0.6VC and the combinations of 0.6VC–0.06La$_2$O$_3$ additions lead to a mixture of stepped triangular prism and near triangular prism (less sharp) WC grains.

Due to the anisotropy growth induced by the additions, most of the WC grains in alloys B–G take the shape of platelet (thin triangular and truncated triangle prism with a length to height ratio of $(10\bar{1}0)$ prism facet more than 2). For WC–10Co alloy without any addition, the WC grains take a truncated multangular prism feature with more than eight crystal planes and a length to height ratio of $(10\bar{1}0)$ prism facet near to 1, which indicates that the difference in the interface energies is small.

LAY et al [14] identified the existence of a thin cubic layer with about 0.5 nm in thickness at the interior of the WC platelet in Ti-doped WC–Co alloy, which suggests that the existence of WC platelets is likely related to the presence of this cubic layer. It was reported that similar cubic layer existed at the boundary between two WC grains and between WC and Co in V/Cr-doped WC–Co alloys [15–17]. Then, we deduce that under the condition of the existence of a high driving force for the grain growth contributed by the nano particle size and a complex transformation, the existence of the cubic layers facilitates the formation of WC platelets. Here, the transformation during the sintering process includes W+C+Co→Co$_x$W$_y$C (eta phase)+C→WC+Co.

YAMAMOTO et al [15] detected that the amount of V content was different in the habit planes (0001) and $(10\bar{1}0)$ of V-doped WC−Co alloy. The concentration of V was several times higher at the (0001) habit plane than at the $(10\bar{1}0)$ one. KAWAKAMI et al [17] detected that the concentration ratios of V or Cr atoms at the (0001) habit plane to the ones at the $(10\bar{1}0)$ habit plane were 3.3 for V in WC−10Co−0.5VC alloy and 1.5 for Cr in WC−10Co−0.9 Cr$_3$C$_2$ alloy prepared in a rapid cooling mode, respectively; the concentration ratios of V or Cr atoms at the (0001) habit plane to the ones at the $(10\bar{1}0)$ habit plane were 5.5 for V and 1.3 for Cr in

WC−10Co−0.5VC−0.9Cr$_3$C$_2$ alloy prepared in a rapid cooling mode, 2.4 for V and 1 for Cr in the same alloy prepared in a usual cooling mode, respectively. YAMAMOTO and KAWAKAMI et al's results on the pronouncedly anisotropic precipitation of V atoms provide a clue to understand the formation of the steps on the WC triangular prisms of alloy C (WC−10Co−0.6VC−0.06La$_2$O$_3$) and alloy F (WC−10Co−0.6VC) with relatively higher V doping amount. The lower addition amount of VC is possibly related to the fact that the combination of 0.4Cr$_3$C$_2$−0.3VC (−0.06La$_2$O$_3$) additions did not result in the formation of easily identified steps.

3.2 Vickers hardness and Palmqvist toughness

Figure 3 shows the combination of Vickers hardness and Palmqvist toughness of alloys A−G. The order from superior to inferior of the combinations of hardness and toughness is as follows: Alloy B > Alloy E > Alloy D > Alloy G > Alloy C > Alloy F. Compared with Alloy A alloy, Alloy B shows a much better combination. Compared with a mixture of platelet triangular and truncated triangle prism WC grains, regular platelet triangular prism WC grains lead to a better combination. La$_2$O$_3$ additions facilitate the improvement of the combination. Rare earth elements have a strong ability to combine the elements with large difference in electronegativity. Therefore, during the sintering process, La can combine with some impurity elements from the raw materials, which can relieve the tendency of the interface segregation of some impurity elements. As a result, the existence of La can possibly cause the local change in the arrangement of the interface atoms and the interface energies. These changes are possibly related to this improvement.

From Figs. 1(c), (f) and Fig. 3, it is known that the formation of easily identified steps on the $\{10\bar{1}0\}$ prismatic facets of WC grains in alloys F and C and the finer average WC grain size are related to an inferior combination of hardness and toughness. Therefore, the addition amount of VC in WC−Co alloys must be optimized. The damage of the crystalline perfection of WC grains resulted from the steps, the decrease in the microstructure homogeneity, as well as the tendency to form an intergranular segregation phase with pronouncedly anisotropic precipitation of V atoms in V-doped WC−Co alloy [18,19] are the reasons behind the inferior combination.

NAM et al [20] reported that the HV$_{30}$ and Palmqvist toughness of (W0.9Ti0.1)C−10Co alloy with (W,Ti)C platelets were 11721 MPa and 13.5 MPa·m$^{1/2}$, respectively. Table 3 shows the composition and properties of H10N and H10P cemented carbides of Sandvik Hard Materials [21]. Compared with our results
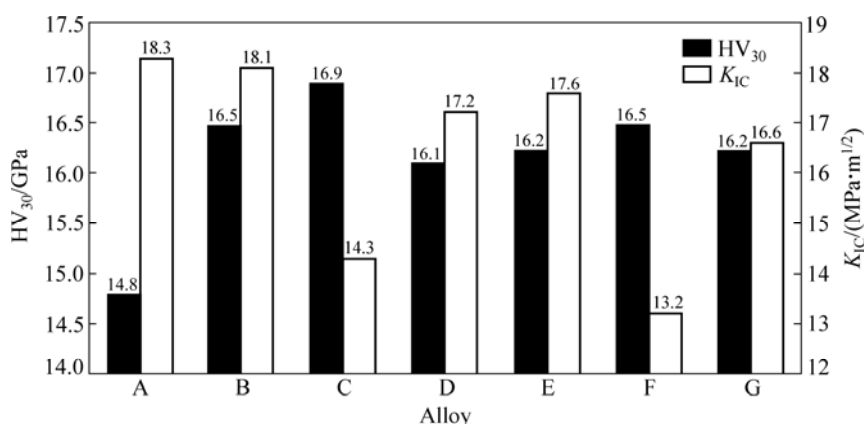
Fig. 3 Double coordinates column plots showing combination of Vickers hardness and Palmqvist toughness of alloys A to G

shown in Fig. 3, it is known that all the alloys A–G show a better combination of hardness and toughness than the one with (W,Ti)C platelets and the counterpart H10N and H10P cemented carbides with similar cobalt content and grain sizes determined by the linear intercept method, and with the conventional WC morphology.

Table 3 Composition and properties of H10N and H10P cemented carbides of Sandvik Hard Materials [21]

Grade	$w(WC)/$ %	$w(Co)/$ %	WC grain size	$HV_{30}/$ GPa	$K_{IC}/$ $(MPa·m^{1/2})$
H10N	90.5	9.5	Medium	13.720	14
H10P	90.5	9.5	Medium-coarse	11.858	17

CHRISTENSEN et al [22] predicted WC grain morphology in WC−Co alloy from interface energies using density-functional theory. It is shown that WC grains are predicted to be hexagonal when the interfaces are assumed to be coherent; and change to a truncated triangular shape where the long prism side lengths are five times longer than the short side lengths, when the interfaces are assumed to be incoherent. Among three types of the interfaces, i.e. coherent, semi-coherent and incoherent, coherent interface shows the highest cohesion. Then, we deduce that the good combination of hardness and toughness is related to the combination of the following facts: 1) the in situ formation of WC crystal without easily identified defects, such as Co inclusions and micro pores within WC grains; 2) the platelet WC morphology which can benefit substantially from the high hardness ratio (1.69) of (0001) basal plane ($HV_{0.05}$=21560 MPa) to the ($10\bar{1}0$) prism facet ($HV_{0.05}$=12740 MPa) [11]; 3) the improvement of the interface cohesion which is influenced by the WC grain morphology; 4) the difference in electronic structure characteristics between WC−Co alloys and (W, Ti)C−Co alloys.

4 Conclusions

1) Cubic carbides and La_2O_3 additions have a strong ability in regulating the WC grain morphological characteristics. The combination of $Cr_3C_2−La_2O_3$ additions leads to regular platelet triangular prism WC grains. Singular Cr_3C_2 and the combinations of $Cr_3C_2−VC$ and $Cr_3C_2−VC−La_2O_3$ additions lead to a mixture of platelet triangular and truncated triangle prism WC grains. Singular VC and the combinations of $VC−La_2O_3$ additions lead to a mixture of stepped platelet triangular prism and near triangular prism WC grains.

2) VC exhibits a strong ability in suppressing the continuous WC grain growth; nevertheless, the ability of VC to control the discontinuous or inhomogeneous WC grain growth is suppressed. As a result, compared with Cr_3C_2, VC additions deteriorate the homogeneity in the microstructure and exaggerate the distribution range of the WC grain sizes, no matter if it is added independently or together with other additions.

3) The order from superior to inferior of the combinations of hardness and toughness is as follows: $WC−10Co−0.6Cr_3C_2−0.06La_2O_3$ > $WC−10Co−0.6Cr_3C_2$ > $WC−10Co−0.4Cr_3C_2−0.3VC−0.06La_2O_3$ > $WC−10Co−0.4Cr_3C_2−0.3VC$ > $WC−10Co−0.6VC−0.06La_2O_3$ > $WC−10Co−0.6VC$. Compared with WC–10Co alloy, $WC−10Co−0.6Cr_3C_2−0.06La_2O_3$ alloy shows a much better combination of hardness and toughness.

4) Compared with a mixture of platelet triangular and truncated triangle prism WC grains, regular and homogeneous platelet triangular prism WC grains lead to a better combination of hardness and toughness. The formation of easily identified steps on the {$10\bar{1}0$} prismatic facets of WC grains can result in an inferior combination. Therefore, the addition amount of VC in WC−Co alloys must be optimized.

References

[1]   MAHMOODAN M, ALIAKBARZADEH H, GHOLAMIPOUR R.

Sintering of WC−10%Co nano powders containing TaC and VC grain growth inhibitors [J]. Transactions of Nonferrous Metals Society of China, 2011, 21(5): 1080−1084.

[2] XIAO Dai-hong, HE Yue-hui, LUO Wei-hong, SONG Min. Effect of VC and NbC additions on microstructure and properties of ultrafine WC−10Co cemented carbides [J]. Transactions of Nonferrous Metals Society of China, 2009, 19(6): 1520−1525.

[3] BONACHE V, SALVADOR M D, FERNÁNDEZ A, BORRELL A. Fabrication of full density near-nanostructured cemented carbides by combination of VC/Cr₃C₂ addition and consolidation by SPS and HIP technologies [J]. International Journal of Refractory Metals and Hard Materials, 2011, 29(2): 202−208.

[4] FANG Z Z, WANG X, RYU T, HWANG K S, SOHN H Y. Synthesis, sintering, and mechanical properties of nanocrystalline cemented tungsten carbide—A review [J]. International Journal of Refractory Metals and Hard Materials, 2009, 27 (2): 288−299.

[5] ZHANG Li, CHEN Shu, WANG Yuan-jie, YU Xian-wang, XIONG Xiang-jun. Tungsten carbide platelet-containing cemented carbide with yttrium containing dispersed phase [J]. Transactions of Nonferrous Metals Society of China, 2008, 18(1): 104−108.

[6] ZHANG Li, WU Hou-ping, CHEN Shu, WANG Zhen-bo, XIONG Xiang-jun. In situ formation of La containing dispersed phase on the sinter skin of La₂O₃ and Cr₃C₂ unitedly doped WC−Co cemented carbide [J]. International Journal of Refractory Metals and Hard Materials, 2009, 27(6): 991−995.

[7] ZHANG Li, CHEN Shu, WU Hou-ping, XIONG Xiang-jun. Migration of La, Ce, Pr, Nd and the in situ formation of Ln₂S₃ and Ln₂O₂S phases on the sinter skin of Cr-mischmetal co-doped WC−Co alloy [C] // ADAMS J P. 2011 International Conference on Tungsten, Refractory and Hardmaterials VIII. San Francisco, USA: Metal Powder Industries Federation, 2011: 03-76−83.

[8] WU Hou-ping, ZHANG Li, YU Xia-wang, CHEN Shu, XIONG Xiang-jun. In-situ formation of RE oxysulfide with self lubricating function during cutting process of cemented carbide tool [J]. The Chinese Journal of Nonferrous Metals, 2009, 19(4): 670−676. (in Chinese)

[9] ZHANG Li, CHEN Shu. Cleaning material for metallurgy furnace, China, CN100462463 C [P]. 2009−02−18. (in Chinese)

[10] SCHUBERT W D, NEUMEISTER H, KINGER G, LUX B. Hardness to toughness relationship of fine-grained WC−Co hardmetals [J]. International Journal of Refractory Metals and Hard Materials, 1998, 16(2): 133−142.

[11] EXNER H E. Physical and chemical nature of cemented carbides [J]. International Metals Reviews, 1979, 24(4): 149−171.

[12] LAY S, ALLIBERT C H, CHRISTENSEN M, WAHNSTRÖM G. Morphology of WC grains in WC−Co alloys [J]. Materials Science and Engineering A, 2008, 486 (1−2): 253−261.

[13] DELANO A, LAY S. Evolution of the WC grain shape in WC−Co alloys during sintering: Cumulated effects of the Cr addition and of the C content [J]. International Journal of Refractory Metals and Hard Materials, 2009, 27(2): 189−197.

[14] LAY S, LOUBRADOU M, SCHUBERT W D. Structural analysis on planar defects formed in WC platelets in Ti-doped WC−Co [J]. Journal of the American Ceramic Society, 2006, 89(10): 3229−3234.

[15] YAMAMOTO T, IKUHARA Y, SAKUM T. High resolution transmission electron microscopy study in VC-doped WC-Co compound [J]. Science and Technology of Advanced Materials, 2000, 1(2): 97−104.

[16] YAMAMOTO T, IKUHARA Y, WATANABE T, SAKUMA T. High resolution microscopy study in Cr₃C₂-doped WC−Co [J]. Journal of Materials Science, 2001, 36 (16): 3885−3890.

[17] KAWAKAMI M, TERADA O, HAYASHI K. Segregation amount of dopants at WC/Co interface in Cr₃C₂ and VC+Cr₃C₂ doped WC–Co submicro-grained cemented carbides[C]//KNERINGER G, RÖDHAMMER P, WILDNER H. 16th International Plansee Seminar. Reutte, Austria: Plansee Holding AG, 2005: 653−667.

[18] LAY S, THIBAULT S H, LOUBRADOU M. Accommodation of the lattice mismatch at the VCₓ−WC interface [J]. Interface Science, 2004, 12(2−3): 187−195.

[19] LAY S, THIBAULT S H, LACKNER A. Location of VC in VC, Cr₃C₂ codoped WC−Co cermets by HREM and EELS [J]. International Journal of Refractory Metals and Hard Materials, 2002, 20(1): 61−69.

[20] NAM H, LIM J, KANG S. Microstructure of (W,Ti)C−Co system containing platelet WC [J]. Materials Science and Engineering A, 2010, 527(27−28): 7163−7167.

[21] BEISS P, RUTHARDT R, WARLIMONT H. Powder metallurgy data. refractory, hard and intermetallic materials [M]. Springer−Verlag, 2002: 13-69−70.

[22] CHRISTENSEN M, WAHNSTRÖM G, LAY S, ALLIBERT C H. Morphology of WC grains in WC−Co alloys: Theoretical determination of grain shape [J]. Acta Materialia, 2007, 55(5): 1515−1521.

立方碳化物和 **La** 添加剂对 **WC−Co** 合金中 **WC** 晶粒形貌以及合金硬度与韧性的影响

张 立[1]，陈 述[2]，程 鑫[1]，吴厚平[1]，马 鋆[1]，熊湘君[1]

1. 中南大学 粉末冶金国家重点实验室，长沙 410083；

2. 长沙矿冶研究院有限责任公司，长沙 410012

摘 要：研究了立方碳化物 Cr₃C₂、VC 以及稀土 La 添加剂对 WC−Co 合金中 WC 晶粒形貌以及合金硬度与韧性的影响。为了强化烧结过程中 WC 晶粒生长的驱动力，采用具有高烧结活性的纳米 W 和纳米 C 为原料。为了获得合金中 WC 晶粒的三维形貌，采用扫描电镜直接观察合金烧结体的自然表面。结果表明，合金添加剂对 WC 晶粒形貌及其粒度分布特征以及合金的硬度与韧性有较大影响。由于均质三角棱柱形板状 WC 晶粒的形成，WC−10Co−0.6Cr₃C₂−0.06La₂O₃ 合金具有极佳的硬度与韧性组合。讨论了合金中 WC 晶粒形貌的调控机制以及合金中 WC 晶粒形貌特征对合金性能的影响。

关键词：硬质合金；稀土；晶粒生长；板状晶 WC；硬度；韧性

(Edited by YANG Hua)